



Neuro-peptide treatment with Cerebrolysin improves the survival of neural stem cell grafts in an APP transgenic model of Alzheimer disease

Edward Rockenstein^{a,1}, Paula Desplats^{a,1}, Kiren Ubhi^a, Michael Mante^a, Jazmin Florio^a, Anthony Adame^a, Stefan Winter^b, Hemma Brandstaetter^b, Dieter Meier^b, Eliezer Masliah^{a,c,*}

^a Department of Neurosciences, University of California San Diego, La Jolla, CA, USA

^b Clinical Research & Pharmacology, EVER Neuro Pharma GmbH, Unterach, Austria

^c Department of Pathology, University of California San Diego, La Jolla, CA, USA


Received 23 December 2014; received in revised form 31 March 2015; accepted 30 April 2015

Available online 9 May 2015

Abstract

Neural stem cells (NSCs) have been considered as potential therapy in Alzheimer's disease (AD) but their use is hampered by the poor survival of grafted cells. Supply of neurotrophic factors to the grafted cells has been proposed as a way to augment survival of the stem cells. In this context, we investigated the utility of Cerebrolysin (CBL), a peptidergic mixture with neurotrophic-like properties, as an adjunct to stem cell therapy in an APP transgenic (tg) model of AD. We grafted murine NSCs into the hippocampus of non-tg and APP tg that were treated systemically with CBL and analyzed after 1, 3, 6 and 9 months post grafting. Compared to vehicle-treated non-tg mice, in the vehicle-treated APP tg mice there was considerable reduction in the survival of the grafted NSCs. Whereas, CBL treatment enhanced the survival of NSCs in both non-tg and APP tg with the majority of the surviving NSCs remaining as neuroblasts. The NSCs of the CBL treated mice displayed reduced numbers of caspase-3 and TUNEL positive cells and increased brain derived neurotrophic factor (BDNF) and furin immunoreactivity. These results suggest that CBL might protect grafted NSCs and as such be a potential adjuvant therapy when combined with grafting.

© 2015 The Authors. Published by Elsevier B.V. This is an open access article under the CC BY-NC-ND license (<http://creativecommons.org/licenses/by-nc-nd/4.0/>).

 This work was partially supported by NIH grant AG05131, AG18440 and by a grant from EVER Pharma.

* Corresponding author at: Department of Neurosciences, University of California, San Diego, La Jolla, CA 92093-0624, USA. Fax: +1 858 534 6232.

E-mail address: emasliah@ucsd.edu (E. Masliah).

¹ These authors contributed equally to this work.

Introduction

The neurogenerative process in patients with Alzheimer's disease (AD) is characterized by synaptic loss (Overk and Masliah, 2014) and loss of cholinergic, glutaminergic and GABA-ergic neurons (DeKosky et al., 1996; Masliah, 1995, 2001; Masliah et al., 2006; Scheff et al., 1990; Terry et al.,

<http://dx.doi.org/10.1016/j.scr.2015.04.008>

1873-5061/© 2015 The Authors. Published by Elsevier B.V. This is an open access article under the CC BY-NC-ND license (<http://creativecommons.org/licenses/by-nc-nd/4.0/>).

1991; Trojanowski et al., 1995). In addition, more recent studies suggest that alterations in adult neurogenesis in the hippocampus might also contribute to the neurodegenerative process in AD (Dong et al., 2004). There is some controversy over whether neurogenesis is increased (Jin et al., 2004) or decreased (Boekhoorn et al., 2006; Li et al., 2008) in AD. Recent studies suggest that apparent increases in neurogenesis in AD patients may be related to glial and vasculature-associated changes (Boekhoorn et al., 2006). Studies in a number of animal models of Familial AD have shown that neurogenesis is reduced (Dong et al., 2004; Donovan et al., 2006; Haughey et al., 2002; Rockenstein et al., 2007).

The mechanisms of neurodegeneration in AD are not completely clear, however progressive accumulation of amyloid beta ($A\beta$) with the formation of oligomers appears to trigger a complex cascade of events that includes activation of several kinases including glycogen synthetase kinase (GSK3 β) and cyclin dependent kinase-5 (CDK5) (Crews and Masliah, 2010; Engmann and Giese, 2009; Shukla et al., 2012) leading to aberrant post-transcriptional modification of the microtubule binding protein—Tau (Gong and Iqbal, 2008). Moreover, other studies suggest that deficient transport or expression of neurotrophic factors (NTF) (e.g., nerve growth factor [NGF], brain derived neurotrophic factor [BDNF]) and their receptors might be involved (Peng et al., 2005; Schindowski et al., 2008; Scott et al., 1995). For this reason, experimental therapies for AD involve reducing the $A\beta$ load, blocking kinases such as GSK3 β and CDK5, reducing Tau and replacement therapies with NTFs (Blurton-Jones et al., 2009; Nagahara et al., 2009; Tuszynski, 2007; Tuszynski et al., 2005).

However, given the advanced clinical stage at which several patients with AD present, alternative therapies are under consideration including replacement therapy with neuronal stem cell grafts. For example, previous studies have shown that neural stem cells (NSC) transferred into the hippocampus of AD transgenic (tg) models improve cognition via BDNF (Nagahara et al., 2009, 2013) and reduce Tau and reelin accumulation in aged Ts65DN model of Down's syndrome (Kern et al., 2011). Moreover, transplantation of NSC derived from induced pluripotent stem cells (iPSC) restore memory in amyloid precursor protein (APP) tg (Fujiwara et al., 2013) and APP/Presenilin-1 (PS1) mice (Zhang et al., 2014a) supporting the notion that treatment with NSCs might be of useful in AD patients. However, a potential problem is the reduced viability of the transplanted cells given the noxious micro-environment in the brain of patients with AD. For example, we have recently shown that under baseline conditions NSC display reduced viability when transplanted into the brains of APP mice, however when these cells are modified to express the $A\beta$ degrading enzyme, neprilysin, the stem cells are more prone to survive (Blurton-Jones et al., 2014). Therefore, adjuvant therapies that enhance survival of grafted stem cells might be important.

Among them, we have considered the potential of combining stem cells with Cerebrolysin™ (CBL) a peptide mixture with neurotrophic-like properties that improves cognition in patients with mild to moderate AD (Alvarez et al., 2006, 2011; Plosker and Gauthier, 2009, 2010; Ruther et al., 1994, 2000). CBL has been shown to be protective in experimental models of excitotoxicity (Veinbergs et al., 2000) and stroke (Onishchenko et al., 2008; Ren et al., 2007; Zhang et al., 2010). In addition, CBL is neurotrophic in APP tg models of AD by promoting

synaptic formation and neurogenesis (Blanchard et al., 2010a,b; Chohan et al., 2011; Rockenstein et al., 2002, 2003, 2005, 2007). The protective effects of CBL in AD-like models involve different mechanisms including regulation of GSK3 β and CDK5 signaling, control of APP metabolism and anti-apoptotic effects mediated by expression of endogenous neurotrophic factors (Ubhi et al., 2013). In this context, the main objective of this study was to investigate whether CBL is capable of enhancing the survival of transplanted NSCs. We found NSC survival progressively declined with age in APP tg mice when compared to controls and that adjuvant therapy with CBL enhanced survival of the BrdU tagged grafted NSC. This study supports the notion that CBL might be a potentially useful adjuvant therapy in combination with NSCs.

Materials and methods

Preparation and CBL testing in mouse cortical neural stem cells

Briefly, as previously described (Crews et al., 2011; Desplats et al., 2012), mouse cortical NSCs were obtained from Millipore. The NSCs were grown on F12/DMEM basal media supplemented with B27 and were kept in proliferative status without induction of neuronal differentiation. Cells were labeled 48 h prior to grafting into the mouse by infection with lentiviral constructs containing the GFP coding sequence at a MOI = 50. Additional pulse labeling with BrdU was carried out 24 h prior to grafting. For in vitro experiments, NSCs were treated with vehicle alone or CBL (5%) and grown in 35 mm dishes and in 6 well plates with a coverslip in the bottom for subsequent ELISA and immunocytochemical studies respectively.

Generation of APP Tg Mice, grafting and Cerebrolysin treatment

For these experiments, hAPP tg mice expressing mutated (Swedish K670M/N671L, London V717I) human(h) APP751 under the control of the mouse (m) Thy-1 promoter (mThy1-hAPP751) (line 41) (Rockenstein et al., 2001) were used. These mice have been extensively characterized (Crews et al., 2010, 2011; Havas et al., 2011; Rockenstein et al., 2011; Spencer et al., 2008) and we have previously shown that these mice display loss of synaptic contacts, defects in neurogenesis, high levels of $A\beta_{1-42}$ production, early amyloid deposition and behavioral deficits (Rockenstein et al., 2003, 2007). Genomic DNA was extracted from tail biopsies and analyzed by PCR amplification, as described previously (Rockenstein et al., 1995). Transgenic lines were maintained by crossing heterozygous tg mice with non-transgenic (non tg) C57BL/6 × DBA/2 F1 breeders. All mice were heterozygous with respect to the transgene.

A total of 128 mice (3 month old) were included in this study (n = 64 non-tg and n = 64 APP tg mice) that were divided into groups of n = 32 corresponding to the post graft time points at which they were analyzed (1, 3, 6 and 9 months). All animals received bilateral stereotaxical injections of the green fluorescent protein (GFP) and BrdU tagged NSC suspension containing 5×10^4 cells/ μ l. Each of the groups (4 groups × n = 32 per time point) included n = 16 non-tg (n = 8 vehicle and n = 8 CBL) and

$n = 16$ APP tg ($n = 8$ vehicle and $n = 8$ CBL) mice. CBL was provided by EVER Pharma in pre-prepared ampoules, each milliliter of CBL contains 215.2 mg of the active CBL concentrate in an aqueous solution (EBEWENeuroPharmaGmbH, 2009). Mass spectrometry analysis of CBL has shown that it is comprised of amino acids (80%) and small (<10 Da) peptides (20%) and previous work had shown that this small peptides mimic the effect of neurotrophic factors including ciliary neurotrophic factor (CNTF), fibroblast growth factor 2 (FGF2) and insulin-like growth factor (IGF) (Chen et al., 2007). Mice were injected daily for the duration of the experiment with saline alone or CBL (i.p., 5 ml/kg, CBL Batch #92382008) for a total of 1, 3, 6 or 9 months. By the end of the experiment for each corresponding group mice were 4, 6, 9 and 12 months old.

All experiments described were approved by the animal subjects committee at the University of California at San Diego (UCSD) and were performed according to NIH guidelines for animal use.

Tissue processing

In accordance with NIH guidelines for the humane treatment of animals, mice were anesthetized with chloral hydrate and flush-perfused transcardially with 0.9% saline. Brains were removed and divided sagittally. The left hemibrain was post-fixed in phosphate-buffered 4% paraformaldehyde (pH 7.4) at 4 °C for 48 h and sectioned at 40 μm with a Vibratome 2000 (Leica, Germany), while the right hemibrain was snap frozen and stored at -70 °C.

Immunohistochemical analysis

Briefly, as previously described (Blurton-Jones et al., 2014; Rockenstein et al., 2007), blind-coded 40 μm thick vibratome sections were immunolabeled with mouse monoclonal antibodies against BrdU (1:500, Millipore), PCNA (1:500, Millipore), GFAP (1:500, Millipore), NeuN (1:500, Millipore), doublecortin (DCX) (1:500, Millipore), Ki-67 (1:100, Santa Cruz), activated caspase-3 (1:1000, Cell Signal), BDNF (1:250, Abcam), NT4 (1:100, Pierce) and furin (1:100, Pierce) followed by horse anti mouse biotinylated secondary antibody and developed with diaminobenzidine and imaged with an Olympus OX54 digital photomicroscope. An additional series of sections were incubated with antibodies against the dendritic marker MAP2 (1:500, Millipore) and $\text{A}\beta$ (1:500, 82E1, IBL). After overnight incubation with the primary antibodies, sections were incubated with FITC-conjugated horse anti-mouse IgG secondary antibody (1:75, Vector Laboratories, Burlingame, CA), transferred to SuperFrost slides (Fisher Scientific, Tustin, CA) and mounted under glass coverslips with anti-fading media (Vector). Moreover, double immunolabeling experiments were performed with the following combinations of antibodies: 1) anti-BrdU and anti-GFP; 2) anti-NeuN and anti-GFP; 3) anti-GFAP and anti-GFP; 4) anti-olig-2 and anti-GFP; 5) anti-BDNF and anti-GFP and 6) anti-Furin and anti-GFP. The BrdU, NeuN, GFAP, olig-2, BDNF and furin were detected with Tyramide Red (NEN) while the GFP was detected via amplification with FITC (green channel). All sections were processed under the same standardized conditions. The immunolabeled sections were imaged with the laser-scanning confocal microscope (LSCM, MRC1024, BioRad, Hercules, CA)

and analyzed as previously described (Rockenstein et al., 2003). Briefly, for each section a total of 8 images at 630 \times were analyzed. For each image a threshold was set utilizing the Image Quant system, the threshold was set within a dynamic range that was consistent for all cases. The levels of pixel intensity or optical density for the area were ascertained with the measure tool of the system. An adjacent un-stained area was used as background to correct against. Area of images analyzed was on average 1024 by 1024 pixels. This area included on average at least 4–5 neurons that were analyzed. The average integrated pixels of optical density for all neurons within that area were estimated and then averaged by the 16 images captured. The average was corrected to the background and expressed as an overall mean by mouse per group. To confirm the specificity of primary antibodies, control experiments were performed where sections were incubated overnight in the absence of primary antibody (deleted) or with preimmune serum or with primary antibody alone.

Unbiased stereology

Stereological methods were used to estimate the number of BrdU immunoreactive cells utilizing an optical fractionator unbiased sampling design (Rockenstein et al., 2007). A total of 4 alternating sections separated by approximately 250 μm containing the hippocampus were outlined using a 4 \times objective attached to an Olympus BX51 microscope. Anatomical nomenclature was based on Paxinos and Franklin (2001). A systematic sampling of the outlined areas was made from a random starting point using StereoInvestigator 8.21.1 software (Micro-BrightField, Cochester, VT). Counts were taken at predetermined intervals ($x = 152$, $y = 152$), and a counting frame (70 \times 70 $\mu\text{m} = 4900 \mu\text{m}^2$) was superimposed on the live image of the tissue sections. Sections were analyzed using a 60 \times 1.4 PlanApo oil-immersion objective with a 1.4 numerical aperture. Section thickness was determined by focusing on the top of the section, zeroing the z-axis and focusing on the bottom of the section. Average section thickness was 18 μm . The dissector height was set at 12 μm . This allowed for a 2- μm top guard zone and at least a 2- μm bottom guard zone. The forbidden zones were never included in the cell counting. Immunoreactive neurons were only counted if the first recognizable profile came into focus within the counting frame. This method allowed for a uniform, systematic, and random design. Differences in stereologic counts were evaluated using the Mann–Whitney test for median differences (GraphPad Prism 4.0c for Macintosh, San Diego, CA). The level of statistical significance was set at p -value < 0.05.

Determination of NTF protein content by ELISA

As previously described (Ubhi et al., 2013), levels of Furin and BDNF were determined in whole brain homogenates by ELISA according to the supplier's protocol (Promega, Madison, WI). The samples were sonicated in a homogenization buffer (20 mM Tris, pH 8, 137 mM NaCl, 1% Nonidet P-40, 1.7 $\mu\text{g}/\text{ml}$ phenylmethylsulfonyl fluoride, 10 $\mu\text{g}/\text{ml}$ aprotinin, 1 $\mu\text{g}/\text{ml}$ leupeptin and 0.5 mM sodium vanadate) at a tissue concentration of 30 $\mu\text{l}/\text{mg}$. An additional control ELISA was performed on whole brain homogenates from non tg mice that had been treated with an amino acid control for CBL.

Statistical analysis

Statistical analysis was performed with the Prism Graph path software package (La Jolla, CA). All results are expressed as mean plus minus SEM. Differences among multiple groups were assessed by one-way ANOVA with post-hoc Dunnett's when comparing to the control group, comparisons among the treatment groups was performed with the Tukey posthoc test. Comparisons between 2 groups were assessed using the two-tailed unpaired Student's t-test.

Results

The reduced survival of grafted NSCs in the brains of APP tg mice is improved by Cerebrolysin treatment

To investigate the survival of grafted cells in APP tg mice, cortical derived mouse NSCs labeled with BrdU and GFP were injected into the hippocampus and mice were analyzed 1, 3, 6 and 9 m post transplantation. Immunocytochemical analysis with an antibody against BrdU showed that the transplanted cells distributed mostly around the CA1 region, the dentate gyrus and the sub-granular zone of the hippocampus (Figs. 1A–C). After 1 month, in the vehicle-treated non-tg mice an average of 13,100 per unit area were found, which was equivalent to approximately to 13.5% of the grafted cells (Figs. 1A, D). After 3 months there was a decline to 5.8% that was stabilized after 6 and 9 months post transplant (6.5%) (Figs. 1B, D). When compared to the non-tg vehicle control group, in the APP tg mice there was a significant reduction in the survival of the grafted cells 1 m post-graft (5100 cells or 5.4%) (Figs. 1B, D). At the later time points only few grafted cells (less than the equivalent to 1%) were found in the vehicle APP tg group (Figs. 1C, D). In the non-tg mice, the numbers of BrdU positive NSCs were similar in the vehicle and CBL treated mice, however after 3, 6 and 9 months survival was higher (14%) in the CBL treated mice compared to vehicle (5.8%) (Fig. 1D). After 1 month in the CBL treated APP tg mice the numbers of BrdU positive NSCs (18,900 or 24%) were above the non-tg groups and the vehicle treated APP mice (Figs. 1A, D). After 3, 6 and 9 months of the transplant the numbers of surviving NSCs were comparable to the non-tg CBL group (12.1%) and above the vehicle-treated APP tg (less than 1%) (Figs. 1B–D). To further corroborate that the BrdU detected cells were the grafted cells, double labeling experiments were performed with antibodies against BrdU and GFP. By confocal microscopy it was observed that the great majority of the GFP positive cells also displayed BrdU reactivity (Figs. 1E, F). These results support the notion that grafted NSC display poor survival in the brains of APP tg mice and that adjuvant treatment with CBL reverts this effect.

Effects of Cerebrolysin and NSC grafting on AD-like neuropathology and endogenous neurogenesis in APP tg mice

To confirm the presence of AD-like neuropathology in the brains of APP tg mice and to evaluate the impact of the combined effects of NSC grafting and CBL treatment sections were immunolabeled with antibodies against A β and GFAP.

As expected compared to the non-tg group the vehicle-treated APP tg mice displayed extensive A β deposition in the neocortex and hippocampus that increased over time (Figs. 2A–C upper panels, D). In contrast, the CBL treated APP tg mice displayed a reduced amyloid deposition that was more prominent 6 and 9 months post-graft and CBL treatment (Figs. 2C upper panels, D). With the antibody against GFAP, in both groups of APP tg mice there was astrogliosis more prominent in the hippocampus than in the neocortex (Figs. 2A–C lower panels). Besides the expected astrogliosis along the injection site no prominent glial reaction was observed as result of the placement of the NSC graft (Figs. 2A–C lower panels). Next we analyzed the effects on neurodegeneration, as we have previously shown that APP tg mice display age related synapto-dendritic loss in the dentate gyrus of the hippocampus (Rockenstein et al., 2002). For this purpose sections were immunolabeled with an antibody against MAP2 and analyzed by confocal microscopy (Fig. 3A). Analysis at 1 month after grafting showed that non-tg and APP tg mice displayed comparable levels of MAP2 immunoreactivity in the molecular layer of the dentate gyrus, although compared to the vehicle, the CBL treated group had slightly higher levels of MAP2 (Figs. 3A, B). However, 3, 6 and 9 m post-grafting the vehicle-treated APP tg mice displayed a significant reduction in the % area of the neuropil covered by MAP2 immunoreactive dendrites (Figs. 3A, B). Compared to vehicle group, grafted APP tg mice displayed levels of MAP2 comparable to the non-tg mice (Fig. 3B).

We have previously shown that in addition to the synapto-dendritic damage, APP tg mice display reduced neurogenesis in the hippocampus (Rockenstein et al., 2007). To evaluate the combined effects of NSC grafting and CBL treatment on endogenous neurogenesis, sections were immunostained with an antibody against double-cortin DCX (Fig. 3C). Analysis at 1 month after grafting showed that compared to vehicle treated non-tg, the APP tg mice displayed a 47% reduction in the number of DCX positive neuroblasts in the subgranular zone of the hippocampus (Figs. 3C, D), in contrast grafted APP tg mice treated with CBL displayed DCX levels comparable to the un-treated non-tg mice (Fig. 3D). After 3, 6 and 9 m post-grafting the vehicle treated APP tg mice displayed further reduction in the numbers of DCX immunoreactive cells (Figs. 3C, D). A similar trend was observed 3 months after grafting in the non-tg mice and in the CBL treated APP tg (Figs. 3C, D). However, at 6 and 9 months numbers of DCX immunoreactive cells leveled (Fig. 3C). Taken together, these studies suggest that the combined effects of enhanced survival of NSC with CBL reduce neurodegeneration in the hippocampus of APP tg mice by ameliorating the degeneration of granular cells and endogenous neuroblasts in the hippocampal dentate gyrus.

Cerebrolysin treatment promotes survival of grafted NSC with no evidence of tumoral proliferation

Given that a subpopulation of grafted NSCs distributes in the dentate gyrus and that there is reduced neurodegeneration and increased endogenous neurogenesis in the granular zone, it is possible that CBL might promote differentiation and integration of grafted NSCs into the hippocampus. To

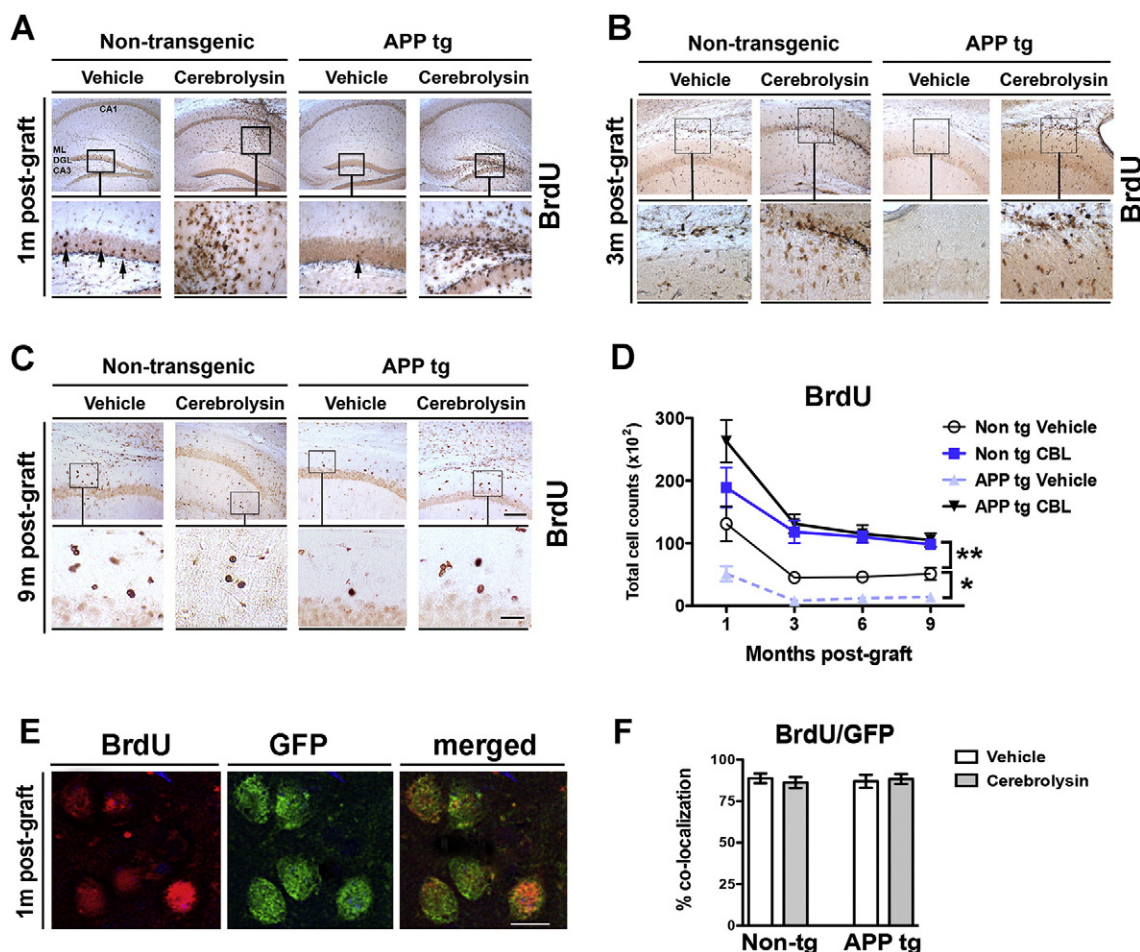


Figure 1 Immunocytochemical analysis of BrdU labeled grafted NSCs in CBL-treated hAPP tg mice. Cortical NSCs labeled with BrdU were transplanted into the hippocampus of non-tg and APP tg mice (3 m/o) treated with vehicle or CBL and immunocytochemical analysis was performed after with vibratome sections 1, 3, 6 and 9 m post graft. (A, B, C) Upper panel representative images at low power (20 \times) 1, 3 and 9 months post graft respectively. Lower panel is higher magnification (400 \times) of the area in the upper panel marked by an open square. Arrows indicate BrdU labeled grafted NSCs distributed along the dentate granular cell layer (DGL). (D) Computer aided image analysis of the numbers of BrdU positive cells in the hippocampus 1, 3, 6 and 9 m post graft. (E, F) Double labeling and confocal microscopy studies for BrdU (red) and GFP (green) in the hippocampus of grafted animals showing high levels of co-localization between the two markers (Bar = 10 μ m). All results are presented as mean \pm SEM, each of the four groups includes n = 32 per time point (n = 16 non-tg [n = 8 vehicle and n = 8 CBL] and n = 16 APP tg [n = 8 vehicle and n = 8 CBL] mice). * = p < 0.05 between vehicle-treated non-tg and APP tg by one-way ANOVA and post Dunnet's. ** = p < 0.05 between vehicle-treated and CBL-treated groups by one-way ANOVA and post hoc Tukey–Kramer. Bar = 250 μ m for low power panel and 50 μ m for high power panel.

investigate this possibility sections were double labeled with antibodies against a mature neuronal marker (NeuN, red) and GFP (to enhance the visualization of the tagged grafted NSCs). Consistent with the BrdU immunocytochemistry studies (Figs. 1A–C), GFP positive cells were identified in the sub-granular zone of the dentate gyrus and in between granular cells (Fig. 4A). At 1 m post grafting, compared to vehicle treated non-tg mice, the vehicle treated APP tg mice displayed a 82% reduction in the numbers of surviving GFP positive NSCs (Figs. 4A, B). In contrast, CBL treatment resulted in an increased number of GFP positive NSCs in the dentate gyrus of non-tg and APP tg mice above the baseline of the controls (Figs. 4A, B). At 3, 6 and 9 months post-grafting there was a mild decline in GFP positive cells in the vehicle treated non-tg mice (Fig. 4A), while in the

vehicle treated APP tg mice the numbers remained very low (Figs. 4A, B). Whereas the CBL treated non-tg and APP tg mice continued to show the presence of GFP positive NSCs above baseline controls (Figs. 4A, B). In all four experimental groups, closer analysis of the immunolabeled sections showed that none of the GFP positive cells were NeuN positive, neither the GFP positive NSCs displayed the presence of neuritic extensions or integration into the dentate gyrus (Fig. 4A arrowheads). Additional double labeling analysis was performed with antibodies against the astroglial marker GFAP (red channel) and GFP (green channel) (Fig. 4C). About 2% of the GFP positive NSCs displayed GFAP immunoreactivity and a glial like morphology (Fig. 4C). Compared to non-tg mice in the APP tg mice at 3 months post grafting there was an increase in the % of cells

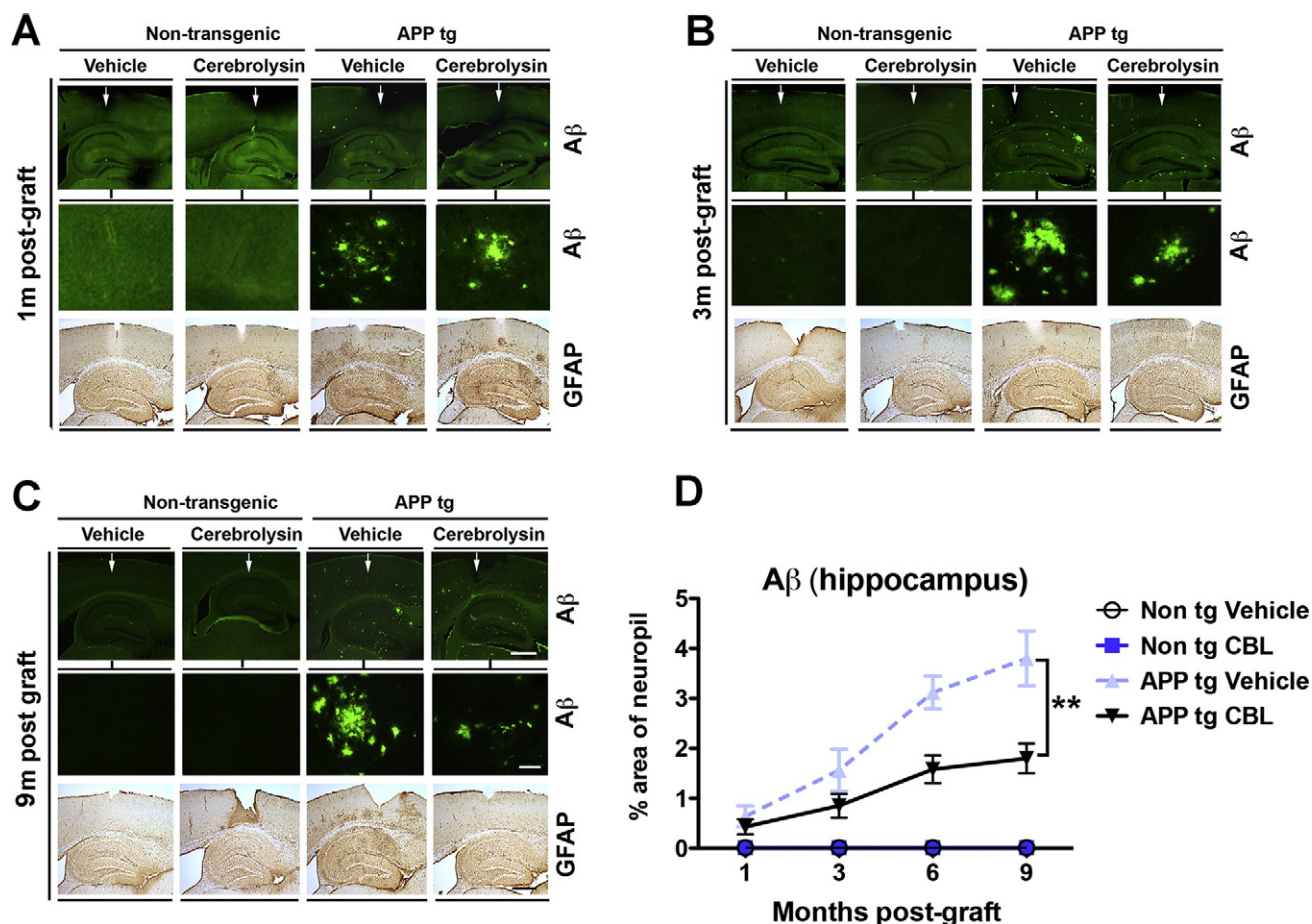


Figure 2 Neuropathological analysis of AD-like pathology in NSC grafted and CBL-treated APP tg mice. Vibratome sections from non-tg and APP tg mice treated with vehicle or CBL and grafted with NSCs were immunolabeled with antibodies against A β (FITC, imaged with the laser scanning confocal microscope) and GFAP (DAB, imaged by digital video microscopy). (A, B, C) Upper panel representative images at low power (20 \times) at 1, 3 and 9 months post graft respectively. Middle panel is higher magnification (400 \times) of the hippocampus dentate gyrus. Arrows indicate site of the injection and tract. Lower panel representative images at low power (20 \times) of the neocortex and hippocampus with an antibody against GFAP. (D) Computer aided image analysis of the A β amyloid load in the hippocampus 1, 3, 6 and 9 m post graft. All results are presented as mean \pm SEM, each of the four groups includes n = 32 per time point (n = 16 non-tg [n = 8 vehicle and n = 8 CBL] and n = 16 APP tg [n = 8 vehicle and n = 8 CBL] mice). ** = p < 0.05 between vehicle-treated and CBL-treated APP tg mice by one-way ANOVA and post hoc Tukey–Kramer. Bar = 250 μ m for low power panel and 50 μ m for high power panel.

displayed GFP and GFAP immunostaining (Figs. 4C, D). No significant effects were detected following CBL treatment (Fig. 4D).

These findings support the notion that CBL might act by enhancing the survival (or proliferation) of grafted NSCs rather than by promoting differentiation. Based on the initial studies showing that starting at 3 months post grafting CBL supports the viability of NSC (Fig. 1B) and to further evaluate the effects of CBL on NSC survival and proliferation sections of mice at the 9 month post-graft were immunolabeled with antibodies against activated caspase-3 and PCNA and stained with a modified version of the TUNEL technique (Fig. 5A). Compared to vehicle treated non-tg mice, the CBL treated mice showed reduced active caspase-3 and TUNEL positive NSCs (Fig. 5B). In contrast, vehicle treated APP tg mice displayed higher numbers of active caspase-3 and TUNEL positive NSCs (Figs. 5B, C), this effect was reversed by CBL treatment (Figs. 5B, C). Occasional PCNA immunoreactivity

was detected in the grafted NSCs; no significant differences were detected among the four groups (Fig. 5D). Likewise, analysis with an antibody against the proliferation marker-Ki-67, at low power no evidence of tumoral proliferation was noted (Fig. 6A), at higher magnification occasional Ki-67 positive cells were noted in the hippocampus (Fig. 6B arrows), treatment with CBL did not reveal an increase in proliferation of NPCs in the grafted area at any of the time points including 9 months post transplantation (Figs. 6B and C). Together these results support the possibility that CBL might enhance the survival of grafted NSCs.

Adjuvant therapy with Cerebrolysin results in increased BDNF and furin levels in grafted NSCs

Since it has been previously shown that CBL increases the conversion of pro-NGF to mature NGF via furin (Ubhi et al.,

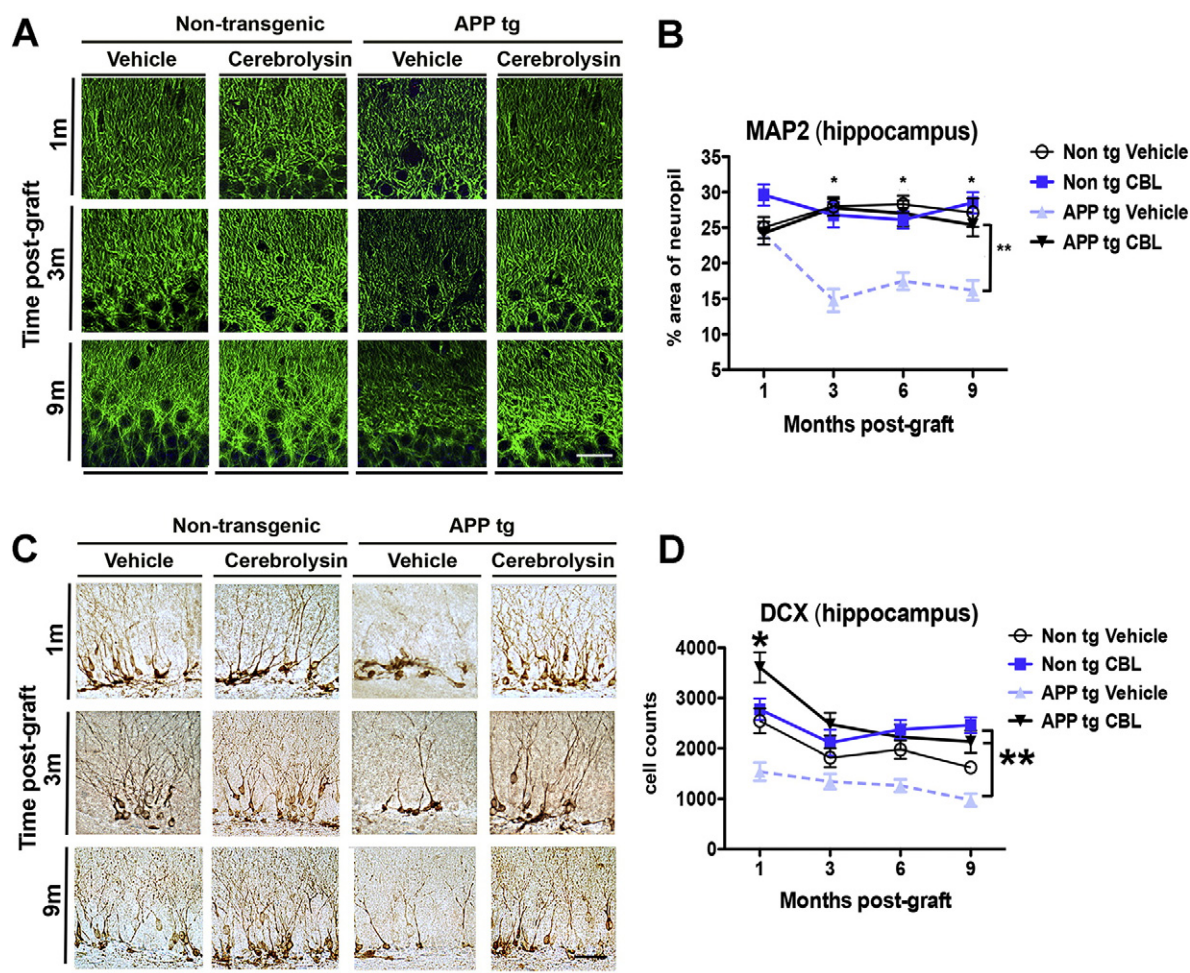


Figure 3 Immunohistochemical analysis of levels of MAP2 and endogenous DCX immunoreactivity in the hippocampus of NSC grafted and CBL-treated APP tg mice. Vibratome sections from non-tg and APP tg mice treated with vehicle or CBL and grafted with NSCs were immunolabeled with an antibody against MAP2 (FITC, imaged with the laser scanning confocal microscope) and doublecortin (DCX) and imaged with the digital video microscope. (A) Representative images at 1, 3 and 9 months post graft respectively of the dendritic arbor (inner molecular layer) of the dentate granular cells. (B) Computer aided image analysis of the % area of the neuropil occupied by MAP2 dendrites at 1, 3, 6 and 9 m post graft. (C) Representative images at 1, 3 and 9 months post graft respectively of the sub-granular zone and dentate gyrus. (D) Computer aided stereological analysis of the estimated DCX+ cell counts at 1, 3, 6 and 9 m post graft. All results are presented as mean \pm SEM, each of the four groups includes $n = 32$ per time point ($n = 16$ non-tg [$n = 8$ vehicle and $n = 8$ CBL] and $n = 16$ APP tg [$n = 8$ vehicle and $n = 8$ CBL] mice). * = $p < 0.05$ between vehicle-treated non-tg mice and vehicle treated APP tg mice by one-way ANOVA and post hoc Dunnett's. ** = $p < 0.05$ between vehicle-treated and CBL-treated APP tg mice by one-way ANOVA and post hoc Tukey–Kramer. Bar = 50 μ m.

2013) and that NSCs can protect adjacent cells via neurotrophic factor production (Blurton-Jones et al., 2009), we analyzed the levels of BDNF, NT4 and furin by immunocytochemistry (Fig. 5E). This study showed that both in non-tg and tg mice levels of BDNF and furin immunostaining were increased in the NSCs of CBL treated mice (Figs. 5E, F, H). No differences were detected for NT4 (Figs. 5E, G). To further confirm that the grafted NSCs were producing BDNF and furin double labeling with GFP was performed (Figs. 5I, K). These studies showed that in the saline treated animals an average of 4% (Figs. 5I, J) and 10% (Figs. 5K, L) of the GFP positive NSCs displayed BDNF or furin immunoreactivity respectively. Treatment with CBL resulted in an increase in the proportion of GFP positive cells displaying BDNF (Figs. 5I, J) or furin immunolabeling (Figs. 5K, L). Further analysis of CBL effects on NSCs was performed in vitro at 0, 4 and 8 DIV.

This study showed that CBL increased BrdU levels (Figs. 7A, B) and decreased TUNEL positive cells at 4 and 8 DIV (Figs. 7C, D). At 4 and 8 DIV the % of MAP2 positive cells increased but no differences were detected between the vehicle and CBL groups (Figs. 7E, F). Moreover, analysis of the levels of BDNF (Fig. 7G) and furin (Fig. 7H) by ELISA with cell lysates at 8 DIV showed a 20–30% increase following CBL treatment (Figs. 7G, H). In conclusion, CBL might enhance the survival of grafted NSC via furin mediated BDNF processing.

Discussion

The present study showed that CBL treatment enhanced the survival of grafted NSCs in APP tg mice. In contrast, in the

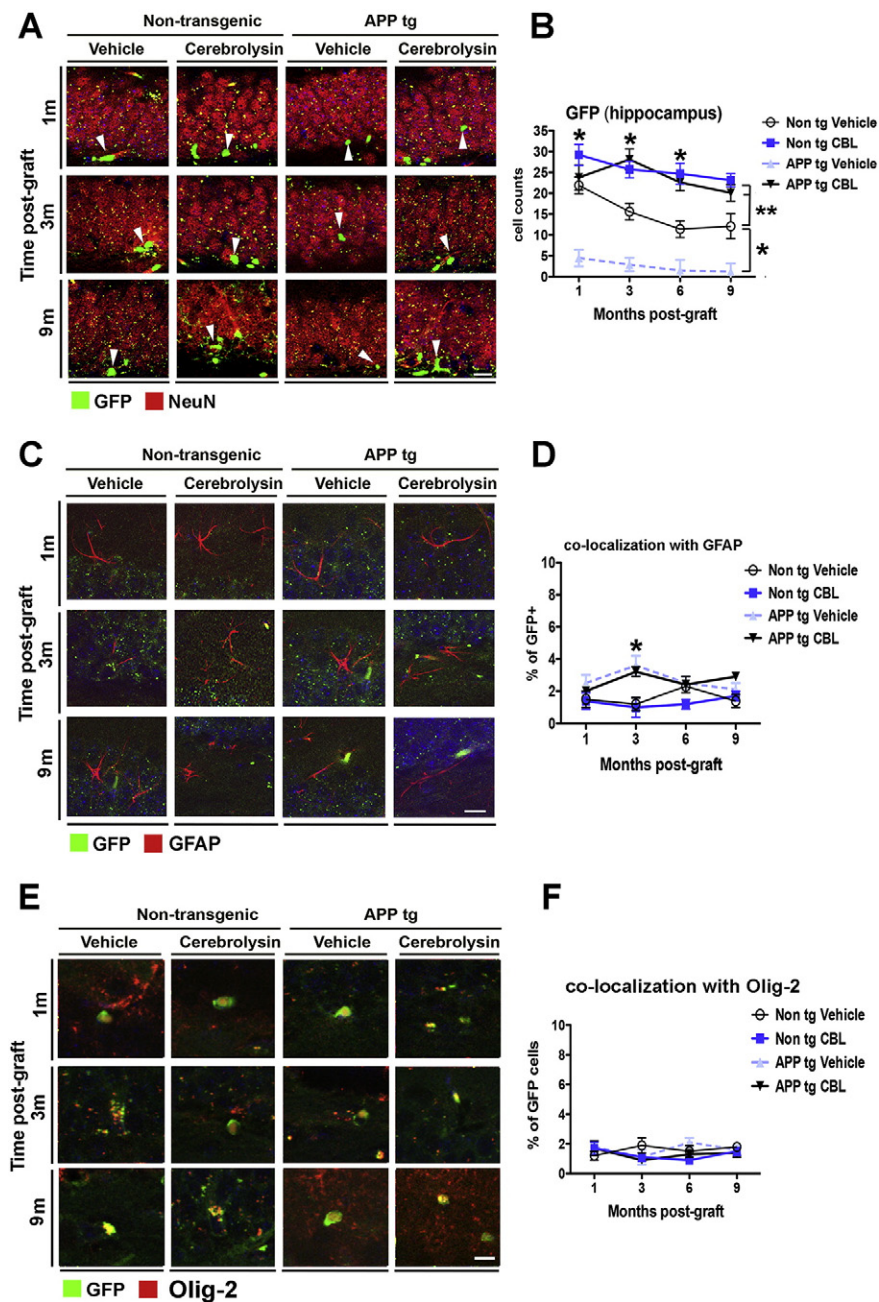


Figure 4 Laser scanning confocal microscopic analysis of neuronal and glial maturation of the grafted NSCs in the hippocampus of CBL-treated APP tg mice. Vibratome sections from non-tg and APP tg mice treated with vehicle or CBL and grafted with NSCs (GFP tagged) were double-immunolabeled with antibodies against NeuN (red) or GFAP (red) and GFP (green) and imaged with the laser scanning confocal microscope. (A) Representative images at 1, 3 and 9 months post graft respectively of the hippocampal dentate gyrus. Images illustrate granular cells (red) and the grafted NSCs (green, arrowheads) that migrated along the sub-granular zone. (B) Computer aided image analysis of the estimated GFP+ cells at 1, 3, 6 and 9 m post graft. (C) Representative images at 1, 3 and 9 months post graft respectively of the hippocampal dentate gyrus. Images illustrate astroglial cells in the dentate gyrus (red) and the grafted NSCs (green) along the sub-granular zone. (D) Computer aided image analysis of the % of co-localization between GFP+ and GFAP cells at 1, 3, 6 and 9 m post graft. (E) Representative images at 1, 3 and 9 months post graft respectively of the hippocampal dentate gyrus. Images illustrate oligodendrocytes (olig-2) in the dentate gyrus (red) and the grafted NSCs (green) along the sub-granular zone. (F) Computer aided image analysis of the % of co-localization between GFP+ and olig-2 cells at 1, 3, 6 and 9 m post graft. All results are presented as mean \pm SEM, each of the four groups includes $n = 32$ per time point ($n = 16$ non-tg [$n = 8$ vehicle and $n = 8$ CBL] and $n = 16$ APP tg [$n = 8$ vehicle and $n = 8$ CBL] mice). * = $p < 0.05$ between vehicle-treated non-tg mice and vehicle treated APP tg mice by one-way ANOVA and post hoc Dunnett's. Bar = 25 μ m.

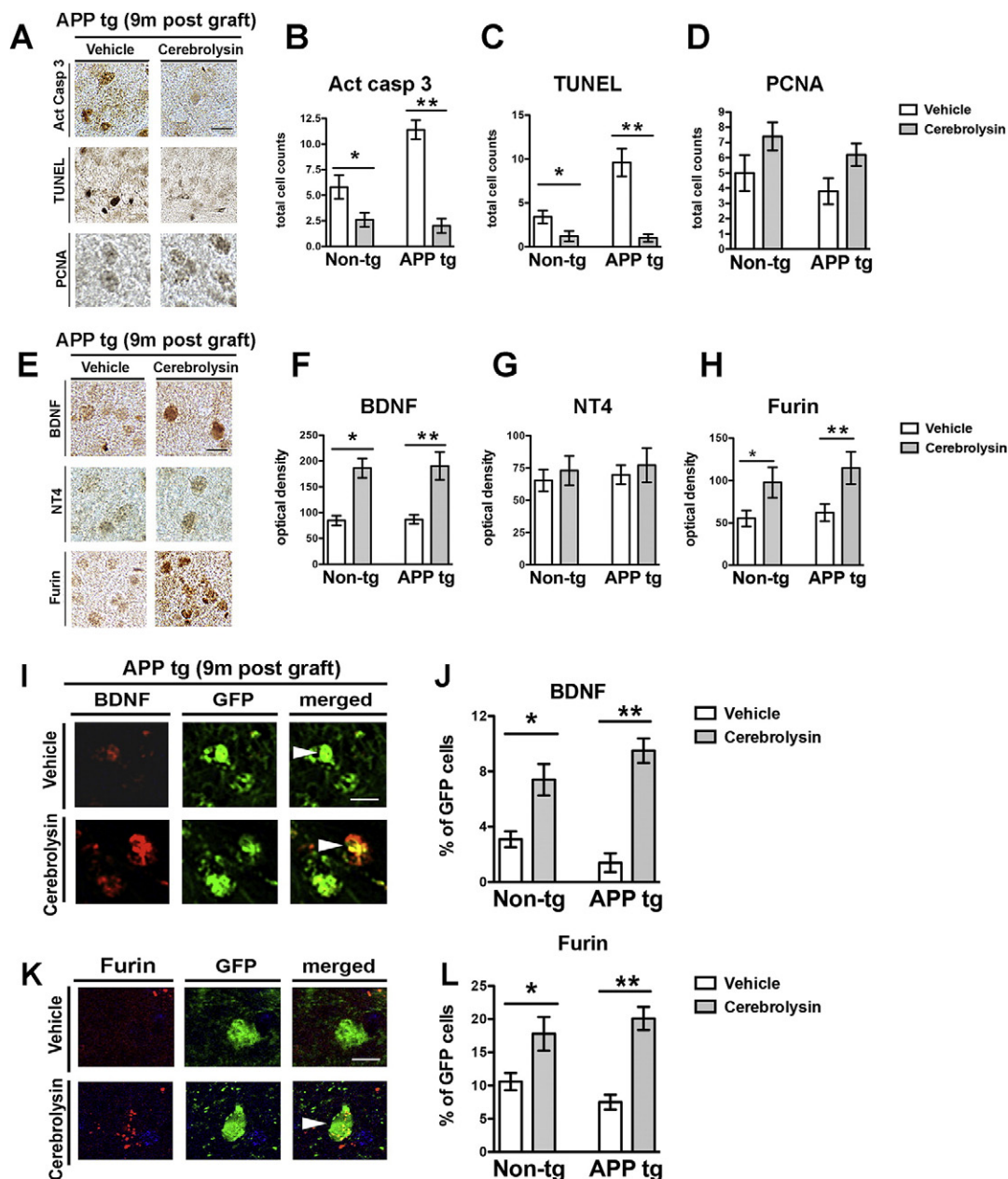


Figure 5 Immunocytochemical and double labeling analysis of markers of cell survival and neurotrophic factors in the grafted NSCs in CBL-treated APP tg mice. Vibratome sections from non-tg and APP tg mice treated with vehicle or CBL and grafted with NSCs were immunolabeled with antibodies against markers of cell death and survival (act casp3, TUNEL and PCNA) and neurotrophic factors (BDNF, NT4 and furin) and imaged with the digital video microscope. (A) Representative images of vehicle and CBL treated APP tg mice at 9 months post graft respectively of the sub-granular zone and dentate gyrus. (B, C, D) Computer aided image analysis of the estimated active caspase 3, TUNEL and PCNA positive cells at 9 months post graft, respectively. (E) Representative images of vehicle and CBL treated APP tg mice at 9 months post graft respectively of the sub-granular zone and dentate gyrus. (F, G, H) Computer aided image analysis of the estimated BDNF, NT4 and Furin positive cells at 9 months post graft respectively. (I) Vibratome sections from non-tg and APP tg mice treated with vehicle or CBL and grafted with NSCs (GFP tagged) were double-immunolabeled with antibodies against BDNF or furin (red) and GFP (green) and imaged with the laser scanning confocal microscope. Representative split images for BDNF (red) and GFP (green) at 9 months post graft of NSC graft in the hippocampal dentate gyrus of vehicle and CBL treated APP tg mice. Images illustrate BDNF co-localization with the GFP tag in the NSCs (arrowhead). (J) Computer aided image analysis of the % of GFP cells that co-localized with BDNF at 9 m post graft. (K) Representative split images for furin (red) and GFP (green) at 9 months post graft of NSCs in the hippocampal dentate gyrus of vehicle and CBL treated APP tg mice. Images illustrate furin co-localization with the GFP tag in the NSCs (arrowhead). (L) Computer aided image analysis of the % of GFP cells that co-localized with furin at 9 m post graft. All results are presented as mean \pm SEM, $n = 16$ non-tg ($n = 8$ vehicle and $n = 8$ CBL) and $n = 16$ APP tg ($n = 8$ vehicle and $n = 8$ CBL) mice. * = $p < 0.05$ between vehicle-treated non-tg mice and CBL treated non-tg mice by one-way ANOVA and post hoc Dunnett's. ** = $p < 0.05$ between vehicle-treated and CBL-treated APP tg mice by one-way ANOVA and post hoc Tukey-Kramer. Bar = 10 μ m.

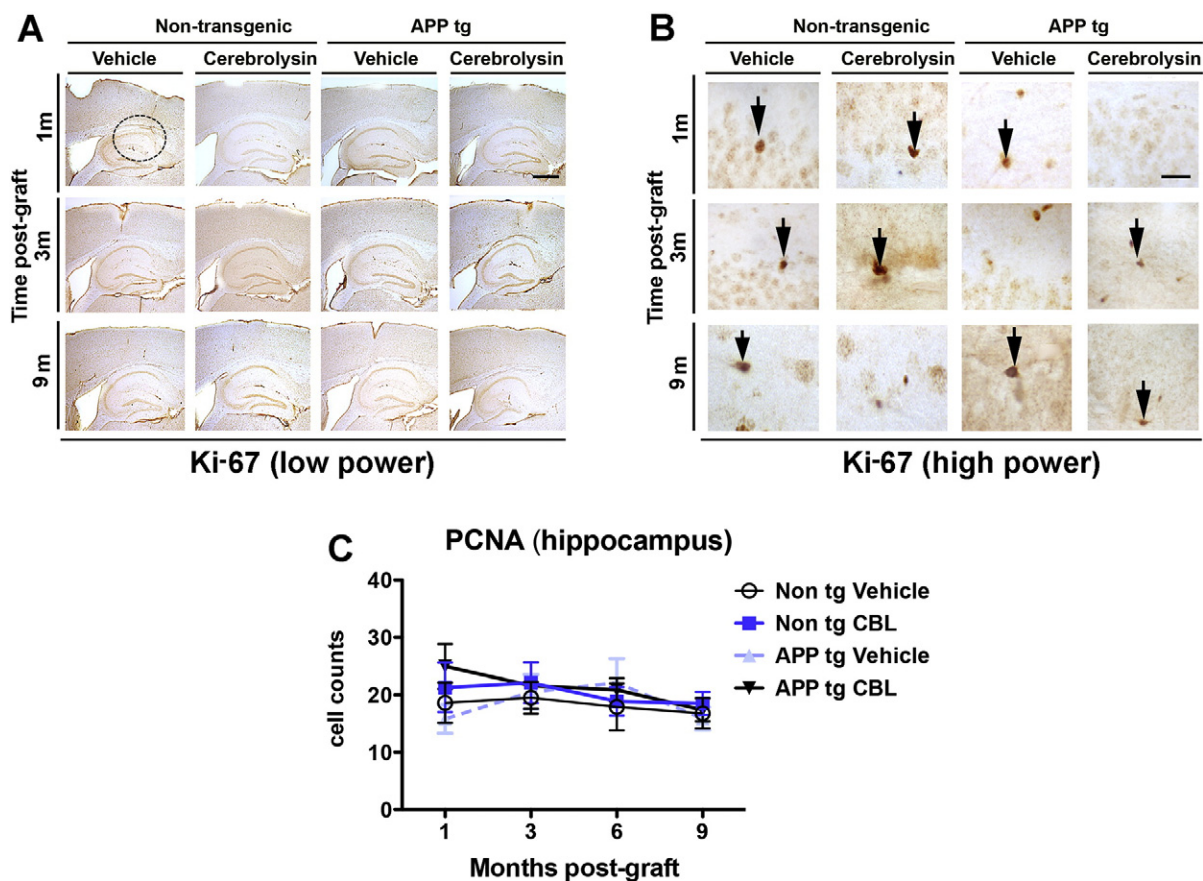


Figure 6 Immunocytochemical analysis of the proliferation marker Ki-67 in the grafted NSCs in CBL-treated APP tg mice. Vibratome sections from non-tg and APP tg mice treated with vehicle or CBL and grafted with NSCs were immunolabeled with an antibody against Ki-67 and imaged with the digital video microscope. (A) Representative low power images (20 \times) of vehicle and CBL treated mice at 1, 3 and 9 months post graft respectively of the neocortex and hippocampus, dotted open circle represent are of graft, bar = 250 μ m. (B) Representative higher power images (630 \times) of Ki-67 positive cells (arrows) for the vehicle and CBL treated mice at 1, 3 and 9 months post graft respectively of the hippocampus of the corresponding site of the graft (dotted open circle in A), bar = 25 μ m. (C) Computer-aided image analysis of the numbers of Ki-67 positive cells in the hippocampus of the non-tg and APP tg mice.

vehicle-treated group there was decreased survival of transplanted neuroblasts that was worse in the APP tg mice. This is consistent with studies showing that the toxic microenvironment in the brain of APP tg mice might compromise the survival of both endogenous and transplanted NSCs. For example, a recent study showed that oligomerized A β 42 promoted the expression of senescence-associated biomarkers p16 and senescence-associated β -galactosidase (SA- β -gal) in adult mouse hippocampal NSCs, and reduced the proliferation and differentiation of these cells in vitro and in APP/PS1 tg mice (He et al., 2013). Moreover, we have observed that extracellular A β triggers apoptosis of transplanted NSCs and that genetically modified NSCs expressing neprilysin reduces amyloid load in APP tg mice and enhances the survival of NSCs and adjacent host neurons (Blurton-Jones et al., 2014), supporting the view of beneficial effects of combined therapy with stem cells.

Previous studies have shown that transfer of rodent NSC into the hippocampus of APP/PS1 tg mice reduces behavioral deficits without changing amyloid β burden (Zhang et al., 2014a) and transplantation of NSCs derived from human iPSC reduce memory deficits in APP mice (Fujiwara et al., 2013).

More recent studies have utilized mesenchymal stem cells and shown CNS trafficking (Danielyan et al., 2014) and neurogenesis (Yan et al., 2014) in APP tg mice. Moreover, other studies have shown that NSC grafting reduced hippocampal Tau and reelin accumulation in aged Ts65Dn Down syndrome mice (Kern et al., 2011) and increased synaptic density in APP tg mice (Blurton-Jones et al., 2009; Zhang et al., 2014b). Together, these studies support the notion that transfer of stem cells is beneficial by promoting neurogenesis and synaptogenesis of endogenous neuronal circuitries. In agreement with these studies, we found that combined NSC and CBL treatment was associated with endogenous neurogenesis and reduced degeneration of the hippocampal dentate gyrus in the APP tg mice.

However, it should be noted that while in previous studies the beneficial effects of stem cell monotherapy were noticed a few weeks post-transplant in our study the combined use of NSC with CBL continued to be helpful after a long period of time. As recently noted, poor viability of transplanted cells could be an important problem associated with stem cell-based therapy for PD (Nakaji-Hirabayashi et al., 2013) and other neurodegenerative disorders. For example, a recent

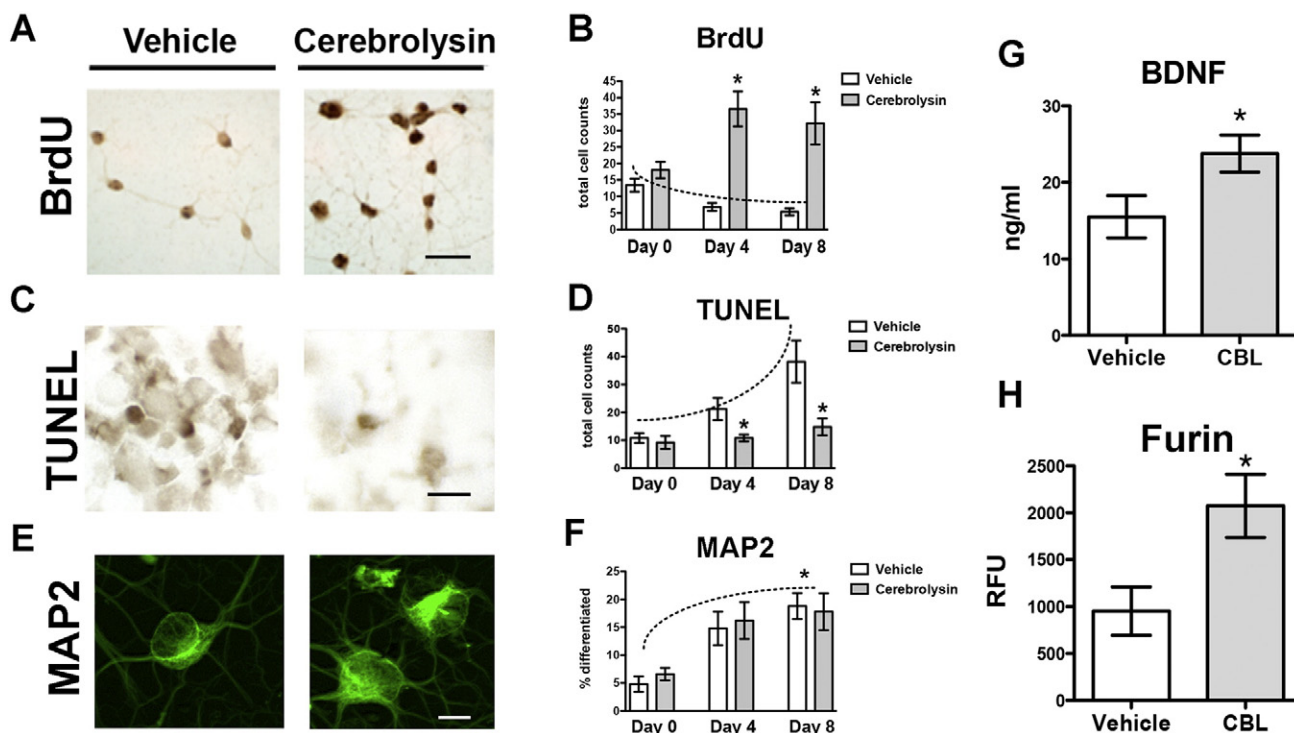


Figure 7 *In vitro* effects of CBL on markers of cell survival and neurotrophic factors in NSCs. Mouse cortical NSCs were grown in coverslips for 0, 4 and 8 days and treated with vehicle or CBL at 5% in media with 1% FBS. (A, C, E) Representative images for NSCs immunostained with an antibody against BrdU, histochemistry for TUNEL or immunostained with an antibody against MAP2 at day 8. (B, D, F) Computer aided image number of cells displaying BrdU, TUNEL or MAP2 reactivity at 0, 4 and 8 DIV. * = $p < 0.05$ between vehicle- and CBL NSCs by two-tailed, Student T-test. Bar = 10 μm . (G, H) ELISA analysis for BDNF and furin in cell lysates at 8 DIV following vehicle or CBL treatment. * = $p < 0.05$ by two-tailed, Student T-test.

study showed that combining a collagen hydrogel incorporating an integrin-binding protein complex as a carrier for neural stem cells improve the viability after transplantation into the striatum (Nakaji-Hirabayashi et al., 2013). Similarly, it has been shown that co-transplantation of GDNF-overexpressing NSCs and fetal neurons ameliorates the motor deficits in a rat model of PD (Deng et al., 2013). Along these lines, for the present study we combined the NSC graft with adjuvant therapy with CBL in an effort to enhance the survival of the transplanted cells. The mechanisms through which CBL might enhance the survival of the grafted cells are not completely clear. One possibility is that CBL might reduce the accumulation of toxic A β species that can potentially damage the grafted NSC. In agreement with this we showed lower levels of A β load following 6 and 9 months of CBL treatment. Moreover previous studies have shown that CBL reduces A β production by reducing maturation of APP mediated by CDK5 and GSK3 β activation (Rockenstein et al., 2006). In addition, we showed that CBL increased furin levels, which in turn resulted in increased processing of pro-BDNF into BDNF in the grafted cells. This is consistent with previous studies showing that CBL might increase levels of NGF perhaps involving the processing of pro-NGF to its mature form (Ubhi et al., 2013). The observed increase in furin levels in CBL-treated APP tg mice is consistent with this hypothesis.

Like pro-NGF (Fahnestock et al., 2001; Peng et al., 2004) pro-BDNF is the precursor protein of BDNF, which is abundant in the hippocampus (Barker, 2009; Bekinschtein et al., 2014;

Lessmann and Brigadski, 2009; West et al., 2014). Pro-BDNF undergoes cleavage by a family of mammalian processing enzymes, including furin (Chen et al., 2015; Fugere and Day, 2005; Seidah and Chretien, 1999). To date there are nine known convertases (Fugere and Day, 2005; Seidah and Chretien, 1999) with furin being the most documented. Moreover, the furin recognition site has been reported to be essential for the proper processing of pro-BDNF to the mature form of BDNF (Lim et al., 2007). Previous studies showed that NSCs are capable of producing BDNF that in turn can protect neighboring host cells (Blurton-Jones et al., 2009; Zhang et al., 2014b). The neuropathological analysis showed that CBL reduced TUNEL and activated caspase-3 in the grafted NSCs, but had no effect of PCNA or Ki-67 at the later time points, supporting the notion of a trophic factor mediated anti-apoptotic effect. However, it is possible that other mechanisms might be at play, including a limited proliferative effect soon after transplantation.

In summary, the results of the present study suggest that CBL is capable of protecting the grafted NSC in an APP tg mouse model and as such be a potential adjuvant therapy when combined with cell based therapy.

Disclosure

Authors Stefan Winter, Hemma Brandstaetter and Dieter Meier are employed by EVER Neuro Pharma who provided the CBL used for this study.

References

- Alvarez, X.A., Cacabelos, R., Laredo, M., Couceiro, V., Sampedro, C., Varela, M., Corzo, L., Fernandez-Novoa, L., Vargas, M., Alexandre, M., et al., 2006. A 24-week, double-blind, placebo-controlled study of three dosages of Cerebrolysin in patients with mild to moderate Alzheimer's disease. *Eur. J. Neurol.* 13, 43–54.
- Alvarez, X.A., Cacabelos, R., Sampedro, C., Alexandre, M., Linares, S., Granizo, E., Doppler, E., Moessler, H., 2011. Efficacy and safety of Cerebrolysin in moderate to moderately severe Alzheimer's disease: results of a randomized, double-blind, controlled trial investigating three dosages of Cerebrolysin. *Eur. J. Neurol.* 18, 59–68.
- Barker, P.A., 2009. Whither proBDNF? *Nat. Neurosci.* 12, 105–106.
- Bekinschtein, P., Cammarota, M., Medina, J.H., 2014. BDNF and memory processing. *Neuropharmacology* 76 (Pt C), 677–683.
- Blanchard, J., Chohan, M.O., Li, B., Liu, F., Iqbal, K., Grundke-Iqbal, I., 2010a. Beneficial effect of a CNTF tetrapeptide on adult hippocampal neurogenesis, neuronal plasticity, and spatial memory in mice. *J. Alzheimers Dis.* 21, 1185–1195.
- Blanchard, J., Wanka, L., Tung, Y.C., Cardenas-Aguayo Mdel, C., LaFerla, F.M., Iqbal, K., Grundke-Iqbal, I., 2010b. Pharmacologic reversal of neurogenic and neuroplastic abnormalities and cognitive impairments without affecting Abeta and tau pathologies in 3xTg-AD mice. *Acta Neuropathol.* 120, 605–621.
- Blurton-Jones, M., Kitazawa, M., Martinez-Coria, H., Castello, N.A., Muller, F.J., Loring, J.F., Yamasaki, T.R., Poon, W.W., Green, K.N., LaFerla, F.M., 2009. Neural stem cells improve cognition via BDNF in a transgenic model of Alzheimer disease. *Proc. Natl. Acad. Sci. U. S. A.* 106, 13594–13599.
- Blurton-Jones, M., Spencer, B., Michael, S., Castello, N.A., Agazaryan, A.A., Davis, J.L., Muller, F.J., Loring, J.F., Masliah, E., LaFerla, F.M., 2014. Neural stem cells genetically modified to express neprilysin reduce pathology in Alzheimer transgenic models. *Stem Cell Res. Ther.* 5, 46.
- Boekhoorn, K., Joels, M., Lucassen, P.J., 2006. Increased proliferation reflects glial and vascular-associated changes, but not neurogenesis in the presenile Alzheimer hippocampus. *Neurobiol. Dis.* 24, 1–14.
- Chen, H., Tung, Y.C., Li, B., Iqbal, K., Grundke-Iqbal, I., 2007. Trophic factors counteract elevated FGF-2-induced inhibition of adult neurogenesis. *Neurobiol. Aging* 28, 1148–1162.
- Chen, Y., Zhang, J., Deng, M., 2015. Furin mediates brain-derived neurotrophic factor upregulation in cultured rat astrocytes exposed to oxygen-glucose deprivation. *J. Neurosci. Res.* 93, 189–194.
- Chohan, M.O., Li, B., Blanchard, J., Tung, Y.C., Heaney, A.T., Rabe, A., Iqbal, K., Grundke-Iqbal, I., 2011. Enhancement of dentate gyrus neurogenesis, dendritic and synaptic plasticity and memory by a neurotrophic peptide. *Neurobiol. Aging* 32, 1420–1434.
- Crews, L., Masliah, E., 2010. Molecular mechanisms of neurodegeneration in Alzheimer's disease. *Hum. Mol. Genet.* 19, R12–R20.
- Crews, L., Adame, A., Patrick, C., Delaney, A., Pham, E., Rockenstein, E., Hansen, L., Masliah, E., 2010. Increased BMP6 levels in the brains of Alzheimer's disease patients and APP transgenic mice are accompanied by impaired neurogenesis. *J. Neurosci. Off. J. Soc. Neurosci.* 30, 12252–12262.
- Crews, L., Patrick, C., Adame, A., Rockenstein, E., Masliah, E., 2011. Modulation of aberrant CDK5 signaling rescues impaired neurogenesis in models of Alzheimer's disease. *Cell Death Dis.* 2, e120.
- Danielyan, L., Beer-Hammer, S., Stolzing, A., Schafer, R., Siegel, G., Fabian, C., Kahle, P., Biedermann, T., Lourhmati, A., Buadze, M., et al., 2014. Intranasal delivery of bone marrow derived mesenchymal stem cells, macrophages, and microglia to the brain in mouse models of Alzheimer's and Parkinson's disease. *Cell Transplant.* 23 (1), S123–S139.
- DeKosky, S.T., Scheff, S.W., Styren, S.D., 1996. Structural correlates of cognition in dementia: quantification and assessment of synapse change. *Neurodegeneration* 5, 417–421.
- Deng, X., Liang, Y., Lu, H., Yang, Z., Liu, R., Wang, J., Song, X., Long, J., Li, Y., Lei, D., Feng, Z., 2013. Co-transplantation of GDNF-overexpressing neural stem cells and fetal dopaminergic neurons mitigates motor symptoms in a rat model of Parkinson's disease. *PLoS One* 8, e80880.
- Desplats, P., Spencer, B., Crews, L., Pathel, P., Morvinski-Friedmann, D., Kosberg, K., Roberts, S., Patrick, C., Winner, B., Winkler, J., Masliah, E., 2012. alpha-Synuclein induces alterations in adult neurogenesis in Parkinson disease models via p53-mediated repression of Notch1. *J. Biol. Chem.* 287, 31691–31702.
- Dong, H., Goico, B., Martin, M., Csernansky, C.A., Bertchume, A., Csernansky, J.G., 2004. Modulation of hippocampal cell proliferation, memory, and amyloid plaque deposition in APPsw (Tg2576) mutant mice by isolation stress. *Neuroscience* 127, 601–609.
- Donovan, M.H., Yazdani, U., Norris, R.D., Games, D., German, D.C., Eisch, A.J., 2006. Decreased adult hippocampal neurogenesis in the PDAPP mouse model of Alzheimer's disease. *J. Comp. Neurol.* 495, 70–83.
- EBEWENeuroPharmaGmbH, 2009. Cerebrolysin® Solution for Injection: Summary of Product Characteristics.
- Engmann, O., Giese, K.P., 2009. Crosstalk between Cdk5 and GSK3beta: implications for Alzheimer's disease. *Front. Mol. Neurosci.* 2, 2.
- Fahnestock, M., Michalski, B., Xu, B., Coughlin, M.D., 2001. The precursor pro-nerve growth factor is the predominant form of nerve growth factor in brain and is increased in Alzheimer's disease. *Mol. Cell. Neurosci.* 18, 210–220.
- Fugere, M., Day, R., 2005. Cutting back on pro-protein convertases: the latest approaches to pharmacological inhibition. *Trends Pharmacol. Sci.* 26, 294–301.
- Fujiwara, N., Shimizu, J., Takai, K., Arimitsu, N., Saito, A., Kono, T., Umehara, T., Ueda, Y., Wakisaka, S., Suzuki, T., Suzuki, N., 2013. Restoration of spatial memory dysfunction of human APP transgenic mice by transplantation of neuronal precursors derived from human iPS cells. *Neurosci. Lett.* 557, B:129–B:134.
- Gong, C.X., Iqbal, K., 2008. Hyperphosphorylation of microtubule-associated protein tau: a promising therapeutic target for Alzheimer disease. *Curr. Med. Chem.* 15, 2321–2328.
- Haughey, N.J., Nath, A., Chan, S.L., Borchard, A.C., Rao, M.S., Mattson, M.P., 2002. Disruption of neurogenesis by amyloid beta-peptide, and perturbed neural progenitor cell homeostasis, in models of Alzheimer's disease. *J. Neurochem.* 83, 1509–1524.
- Havas, D., Hutter-Paier, B., Ubhi, K., Rockenstein, E., Crailsheim, K., Masliah, E., Windisch, M., 2011. A longitudinal study of behavioral deficits in an AbetaPP transgenic mouse model of Alzheimer's disease. *J. Alzheimers Dis.* 25, 231–243.
- He, N., Jin, W.L., Lok, K.H., Wang, Y., Yin, M., Wang, Z.J., 2013. Amyloid-beta(1–42) oligomer accelerates senescence in adult hippocampal neural stem/progenitor cells via formylpeptide receptor 2. *Cell Death Dis.* 4, e924.
- Jin, K., Peel, A.L., Mao, X.O., Xie, L., Cottrell, B.A., Henshall, D.C., Greenberg, D.A., 2004. Increased hippocampal neurogenesis in Alzheimer's disease. *Proc. Natl. Acad. Sci. U. S. A.* 101, 343–347.
- Kern, D.S., Maclean, K.N., Jiang, H., Synder, E.Y., Sladek Jr., J.R., Bjugstad, K.B., 2011. Neural stem cells reduce hippocampal tau and reelin accumulation in aged Ts65Dn Down syndrome mice. *Cell Transplant.* 20, 371–379.
- Lessmann, V., Brigadski, T., 2009. Mechanisms, locations, and kinetics of synaptic BDNF secretion: an update. *Neurosci. Res.* 65, 11–22.
- Li, B., Yamamori, H., Tatebayashi, Y., Shafit-Zagardo, B., Tanimukai, H., Chen, S., Iqbal, K., Grundke-Iqbal, I., 2008. Failure of neuronal maturation in Alzheimer disease dentate gyrus. *J. Neuropathol. Exp. Neurol.* 67, 78–84.

- Lim, K.C., Tyler, C.M., Lim, S.T., Giuliano, R., Federoff, H.J., 2007. Proteolytic processing of proNGF is necessary for mature NGF regulated secretion from neurons. *Biochem. Biophys. Res. Commun.* 361, 599–604.
- Masliah, E., 1995. Mechanisms of synaptic dysfunction in Alzheimer's disease. *Histol. Histopathol.* 10, 509–519.
- Masliah, E., 2001. Recent advances in the understanding of the role of synaptic proteins in Alzheimer's Disease and other neurodegenerative disorders. *J. Alzheimers Dis.* 3, 121–129.
- Masliah, E., Crews, L., Hansen, L., 2006. Synaptic remodeling during aging and in Alzheimer's disease. *J. Alzheimers Dis.* 9, 91–99.
- Nagahara, A.H., Merrill, D.A., Coppola, G., Tsukada, S., Schroeder, B.E., Shaked, G.M., Wang, L., Blesch, A., Kim, A., Conner, J.M., et al., 2009. Neuroprotective effects of brain-derived neurotrophic factor in rodent and primate models of Alzheimer's disease. *Nat. Med.* 15, 331–337.
- Nagahara, A.H., Mateling, M., Kovacs, I., Wang, L., Eggert, S., Rockenstein, E., Koo, E.H., Masliah, E., Tuszynski, M.H., 2013. Early BDNF treatment ameliorates cell loss in the entorhinal cortex of APP transgenic mice. *J. Neurosci. Off. J. Soc. Neurosci.* 33, 15596–15602.
- Nakaji-Hirabayashi, T., Kato, K., Iwata, H., 2013. In vivo study on the survival of neural stem cells transplanted into the rat brain with a collagen hydrogel that incorporates laminin-derived polypeptides. *Bioconjug. Chem.* 24, 1798–1804.
- Onishchenko, L.S., Gaikova, O.N., Yanishevskii, S.N., 2008. Changes at the focus of experimental ischemic stroke treated with neuroprotective agents. *Neurosci. Behav. Physiol.* 38, 49–54.
- Overk, C.R., Masliah, E., 2014. Pathogenesis of synaptic degeneration in Alzheimer's disease and Lewy body disease. *Biochem. Pharmacol.* 88, 508–516.
- Paxinos, G., Franklin, K., 2001. *The Mouse Brain in Stereotaxic Coordinates*. Second ed. Academic Press, San Diego.
- Peng, S., Wu, J., Mufson, E.J., Fahnstock, M., 2004. Increased proNGF levels in subjects with mild cognitive impairment and mild Alzheimer disease. *J. Neuropathol. Exp. Neurol.* 63, 641–649.
- Peng, S., Wu, J., Mufson, E.J., Fahnstock, M., 2005. Precursor form of brain-derived neurotrophic factor and mature brain-derived neurotrophic factor are decreased in the pre-clinical stages of Alzheimer's disease. *J. Neurochem.* 93, 1412–1421.
- Plosker, G.L., Gauthier, S., 2009. Cerebrolysin: a review of its use in dementia. *Drugs Aging* 26, 893–915.
- Plosker, G.L., Gauthier, S., 2010. Spotlight on cerebrolysin in dementia. *CNS Drugs* 24, 263–266.
- Ren, J., Sietsma, D., Qiu, S., Moessler, H., Finklestein, S.P., 2007. Cerebrolysin enhances functional recovery following focal cerebral infarction in rats. *Restor. Neurol. Neurosci.* 25, 25–31.
- Rockenstein, E.M., McConlogue, L., Tan, H., Power, M., Masliah, E., Mucke, L., 1995. Levels and alternative splicing of amyloid beta protein precursor (APP) transcripts in brains of APP transgenic mice and humans with Alzheimer's disease. *J. Biol. Chem.* 270, 28257–28267.
- Rockenstein, E., Mallory, M., Mante, M., Sisk, A., Masliah, E., 2001. Early formation of mature amyloid-beta protein deposits in a mutant APP transgenic model depends on levels of Abeta(1–42). *J. Neurosci. Res.* 66, 573–582.
- Rockenstein, E., Mallory, M., Mante, M., Alford, M., Windisch, M., Moessler, H., Masliah, E., 2002. Effects of Cerebrolysin on amyloid-beta deposition in a transgenic model of Alzheimer's disease. *J. Neural Transm. Suppl.* 327–336.
- Rockenstein, E., Adame, A., Mante, M., Moessler, H., Windisch, M., Masliah, E., 2003. The neuroprotective effects of Cerebrolysin in a transgenic model of Alzheimer's disease are associated with improved behavioral performance. *J. Neural Transm.* 110, 1313–1327.
- Rockenstein, E., Adame, A., Mante, M., Larrea, G., Crews, L., Windisch, M., Moessler, H., Masliah, E., 2005. Amelioration of the cerebrovascular amyloidosis in a transgenic model of Alzheimer's disease with the neurotrophic compound cerebrolysin. *J. Neural Transm.* 112, 269–282.
- Rockenstein, E., Torrance, M., Mante, M., Adame, A., Paulino, A., Rose, J.B., Crews, L., Moessler, H., Masliah, E., 2006. Cerebrolysin decreases amyloid-beta production by regulating amyloid protein precursor maturation in a transgenic model of Alzheimer's disease. *J. Neurosci. Res.* 83, 1252–1261.
- Rockenstein, E., Mante, M., Adame, A., Crews, L., Moessler, H., Masliah, E., 2007. Effects of Cerebrolysin on neurogenesis in an APP transgenic model of Alzheimer's disease. *Acta Neuropathol.* 113, 265–275.
- Rockenstein, E., Ubhi, K., Pham, E., Michael, S., Doppler, E., Novak, P., Inglis, C., Mante, M., Adame, A., Alvarez, X.A., et al., 2011. Beneficial effects of a neurotrophic peptidergic mixture persist for a prolonged period following treatment interruption in a transgenic model of Alzheimer's disease. *J. Neurosci. Res.* 89, 1812–1821.
- Ruther, E., Ritter, R., Apecechea, M., Freitag, S., Windisch, M., 1994. Efficacy of Cerebrolysin in Alzheimer's disease. In: Jellinger, K., Ladurner, G., Windisch, M. (Eds.), *New Trends in the Diagnosis and Therapy of Alzheimer's Disease*. Springer-Verlag, Vienna, pp. 131–141.
- Ruther, E., Ritter, R., Apecechea, M., Freitag, S., Gmeinbauer, R., Windisch, M., 2000. Sustained improvements in patients with dementia of Alzheimer's type (DAT) 6 months after termination of Cerebrolysin therapy. *J. Neural Transm.* 107, 815–829.
- Scheff, S., DeKosky, S., Price, D., 1990. Quantitative assessment of cortical synaptic density in Alzheimer's disease. *Neurobiol. Aging* 11, 29–37.
- Schindowski, K., Belarbi, K., Buee, L., 2008. Neurotrophic factors in Alzheimer's disease: role of axonal transport. *Genes Brain Behav.* 7 (Suppl. 1), 43–56.
- Scott, S.A., Mufson, E.J., Weingartner, J.A., Skau, K.A., Crutcher, K.A., 1995. Nerve growth factor in Alzheimer's disease: increased levels throughout the brain coupled with declines in nucleus basalis. *J. Neurosci. Off. J. Soc. Neurosci.* 15, 6213–6221.
- Seidah, N.G., Chretien, M., 1999. Proprotein and prohormone convertases: a family of subtilases generating diverse bioactive polypeptides. *Brain Res.* 848, 45–62.
- Shukla, V., Skuntz, S., Pant, H.C., 2012. Deregulated Cdk5 activity is involved in inducing Alzheimer's disease. *Arch. Med. Res.* 43, 655–662.
- Spencer, B., Marr, R.A., Rockenstein, E., Crews, L., Adame, A., Potkar, R., Patrick, C., Gage, F.H., Verma, I.M., Masliah, E., 2008. Long-term neprilysin gene transfer is associated with reduced levels of intracellular Abeta and behavioral improvement in APP transgenic mice. *BMC Neurosci.* 9, 109.
- Terry, R., Masliah, E., Salmon, D., Butters, N., DeTeresa, R., Hill, R., Hansen, L., Katzman, R., 1991. Physical basis of cognitive alterations in Alzheimer disease: synapse loss is the major correlate of cognitive impairment. *Ann. Neurol.* 30, 572–580.
- Trojanowski, J.Q., Shin, R.W., Schmidt, M.L., Lee, V.M., 1995. Relationship between plaques, tangles, and dystrophic processes in Alzheimer's disease. *Neurobiol. Aging* 16, 335–340 (discussion 341–335).
- Tuszynski, M.H., 2007. Nerve growth factor gene delivery: animal models to clinical trials. *Dev. Neurobiol.* 67, 1204–1215.
- Tuszynski, M.H., Thal, L., Pay, M., Salmon, D.P., U HS, Bakay, R., Patel, P., Blesch, A., Vahlsing, H.L., Ho, G., et al., 2005. A phase 1 clinical trial of nerve growth factor gene therapy for Alzheimer disease. *Nat. Med.* 11, 551–555.
- Ubhi, K., Rockenstein, E., Vazquez-Roque, R., Mante, M., Inglis, C., Patrick, C., Adame, A., Fahnstock, M., Doppler, E., Novak, P., et al., 2013. Cerebrolysin modulates pronerve growth factor/nerve growth factor ratio and ameliorates the cholinergic deficit in a transgenic model of Alzheimer's disease. *J. Neurosci. Res.* 91, 167–177.

- Veinbergs, I., Mante, M., Mallory, M., Masliah, E., 2000. Neurotrophic effects of Cerebrolysin in animal models of excitotoxicity. *J. Neural Transm. Suppl.* 59, 273–280.
- West, A.E., Pruunsild, P., Timmusk, T., 2014. Neurotrophins: transcription and translation. *Handb. Exp. Pharmacol.* 220, 67–100.
- Yan, Y., Ma, T., Gong, K., Ao, Q., Zhang, X., Gong, Y., 2014. Adipose-derived mesenchymal stem cell transplantation promotes adult neurogenesis in the brains of Alzheimer's disease mice. *Neural Regen. Res.* 9, 798–805.
- Zhang, C., Chopp, M., Cui, Y., Wang, L., Zhang, R., Zhang, L., Lu, M., Szalad, A., Doppler, E., Hitzl, M., Zhang, Z.G., 2010. Cerebrolysin enhances neurogenesis in the ischemic brain and improves functional outcome after stroke. *J. Neurosci. Res.* 88, 3275–3281.
- Zhang, W., Wang, P.J., Sha, H.Y., Ni, J., Li, M.H., Gu, G.J., 2014a. Neural stem cell transplants improve cognitive function without altering amyloid pathology in an APP/PS1 double transgenic model of Alzheimer's disease. *Mol. Neurobiol.* 50, 423–437.
- Zhang, W., Wang, G.M., Wang, P.J., Zhang, Q., Sha, S.H., 2014b. Effects of neural stem cells on synaptic proteins and memory in a mouse model of Alzheimer's disease. *J. Neurosci. Res.* 92, 185–194.